Published in final edited form as:
Circ Arrhythm Electrophysiol. 2012 December ; 5(6): 1081–1090. doi:10.1161/CIRCEP.112.970699.

Myocardial Structural Associations with Local Electrograms: A Study of Post-Infarct Ventricular Tachycardia Pathophysiology and Magnetic Resonance Based Non-Invasive Mapping

Takeshi Sasaki, MD, PhD[1], **Christopher F. Miller, MS**[1], **Rozann Hansford, RN, MPH**[1], **Juemin Yang, PhD**[2], **Brian S. Caffo, PhD**[2], **Menekhem M. Zviman, PhD**[1], **Charles A. Henrikson, MD, MPH**[3], **Joseph E. Marine, MD**[1], **David Spragg, MD**[1], **Alan Cheng, MD**[1], **Harikrishna Tandri, MD**[1], **Sunil Sinha, MD**[1], **Aravindan Kolandaivelu, MD**[1], **Stefan L. Zimmerman, MD**[4], **David A. Bluemke, MD, PhD**[5], **Gordon F. Tomaselli, MD**[1], **Ronald D. Berger, MD, PhD**[1], **Hugh Calkins, MD**[1], **Henry R. Halperin, MD**[1,6], and **Saman Nazarian, MD, PhD**[1]

[1]Dept of Medicine/Cardiology, Johns Hopkins University School of Medicine, Baltimore, MD

[2]Dept of Biostatistics, Johns Hopkins Bloomberg School of Public Health, Baltimore, MD

[3]Dept of Medicine/Cardiology, Oregon Health Sciences University, Portland, OR

[4]Dept of Medicine/Radiology & Radiological Science, Johns Hopkins University, Baltimore

[5]Radiology & Imaging Sciences, NIH Clinical Center, National Institute of Biomedical Imaging and Bioengineering, Bethesda, MD

[6]Dept of Medicine, Radiology & Biomedical Engineering, Johns Hopkins University School of Medicine, Baltimore, MD

Abstract

Background—The association of scar on late-gadolinium enhancement cardiac magnetic resonance (LGE-CMR) with local electrograms on electroanatomic mapping (EAM) has been investigated. We aimed to quantify these associations to gain insights regarding LGE-CMR image characteristics of tissues and critical sites that support post-infarct ventricular tachycardia (VT).

Methods and Results—LGE-CMR was performed in 23 patients with ischemic cardiomyopathy before VT ablation. Left ventricular wall thickness and post-infarct scar thickness were measured in each of 20 sectors per LGE-CMR short-axis plane. EAM points were retrospectively registered to the corresponding LGE-CMR images. Multivariable regression analysis, clustered by patient, revealed significant associations between left ventricular wall thickness, post infarct scar thickness, and intramural scar location on LGE-CMR, and local endocardial electrogram bipolar/unipolar voltage, duration, and deflections on EAM. Antero-posterior and septal/lateral scar localization was also associated with bipolar and unipolar voltage. Anti-arrhythmic drug use was associated with electrogram duration. Critical sites of post-infarct VT were associated with >25% scar transmurality and slow conduction sites with >40 msec stimulus-QRS time were associated with >75% scar transmurality.

Address for Correspondence: Takeshi Sasaki, MD, Division of Cardiology, Johns Hopkins University, Carnegie 592C, 600 N. Wolfe Street, Baltimore, MD 21287, Tel: 443-614-2751, Fax: 410-502-4854, tsasaki1@jhu.edu.

Conflict of Interest Disclosures: Dr. Nazarian has received honoraria for lectures from St. Jude Medical Inc., Boston Scientific Inc., and Biotronic Inc. Dr. Nazarian is on the MRI advisory board to Medtronic Inc., and is a scientific advisor to Biosense-Webster Inc. Dr. Halperin has received research grant and consultant fees from Zoll Circulation Inc., and has ownership interests in IMRICOR Medical Systems Inc. Dr. Calkins has received honoraria from Biosense-Webster Inc. and Medtronic Inc. Dr. Berger has received research grants from St. Jude Medical Inc. and Medtronic Inc. and consultant fees from Boston Scientific Crop. and Cameron Health Inc. The Johns Hopkins University Conflict of Interest Committee manages all commercial arrangements.

Conclusions—Critical sites for maintenance of post-infarct VT are confined to areas with >25% scar transmurality. Our data provides insights into the structural substrates for delayed conduction and VT, and may reduce procedural time devoted to substrate mapping, overcome limitations of invasive mapping due to sampling density, and enhance magnetic resonance based ablation by feature extraction from complex images.

Keywords

ischemic heart disease; magnetic resonance imaging; mapping; ventricular tachycardia; late gadolinium enhancement

Introduction

Catheter ablation is increasingly used as an adjunct to implantable cardioverter defibrillators (ICD) and medical therapy for management of ventricular tachycardia (VT) in patients with ischemic and nonischemic cardiomyopathy.[1–6] Due to hemodynamic instability, the majority of scar-related VTs are unmappable during tachycardia. Consequently, significant progress has been made in substrate-guided ablation based on electrogram (EGM) characteristics as surrogates of the scar substrate on electroanatomic maps (EAMs) obtained during sinus rhythm. The EGM characteristics central to identification of tissues that participate in VT circuits include low EGM voltage and fractionated or isolated potentials.

Late gadolinium enhancement (LGE) on cardiac magnetic resonance (CMR) can accurately characterize the transmural extent, location, and configuration of scar.[7, 8] Previous reports have shown that scar extent on LGE-CMR is significantly associated with VT inducibility and prognosis in patients with structural heart disease.[9, 10] Additionally, scar transmurality, defined as the ratio of post-infarct scar thickness (PI-ST) to left ventricular wall thickness (LV-WT), has been associated with EGM characteristics on EAM.[11–19] Local EGMs reflect the characteristics of scar as well as total myocardium near the catheter, intuitively measured as the absolute values of local PI-ST and LV-WT rather than their ratio. Therefore, we sought to (a) examine the association of scar transmurality with EGM characteristics and critical sites that support post-infarct VT, and (b) quantify the independent association of absolute PI-ST and LV-WT with EGM characteristics, for non-invasive creation of EAM based on pre-procedural LGE-CMR.

Methods

Study patients

The Johns Hopkins Institutional Review Board approved the study protocol. All patients provided written informed consents. LGE-CMR images were acquired prior to catheter ablation in 23 patients with ischemic cardiomyopathy and VT.

CMR studies

CMR was performed with a 1.5T magnetic resonance scanner (Avanto, Siemens, Erlangen, Germany). In patients with ICD systems, risks of CMR were explained, and images were obtained using our established safety protocol.[20, 21] Short-axis cine steady-state free precession gradient-echo images (Cine-CMR) were obtained (echo time 1.1–1.6 ms, repetition time 2.5–3.8 ms, average in-plane resolution 1.4×1.4 mm; flip angle 15–60°; temporal resolution 40–45ms) in contiguous 8 mm planes from base to apex. Fifteen minutes after intravenous injection of 0.2mmol/kg gadodiamide, short-axis LGE-CMR images were obtained using an inversion-recovery fast-gradient-echo pulse sequence (echo time 1.3–3.9 ms, repetition time 5.4–8.3 ms, average in-plane resolution 1.5×2.0 mm; 8 mm

slice thickness). Inversion times (range 175–300 ms) were optimized to maximize conspicuity of myocardial areas with delayed enhancement.

CMR Image Analysis

QMass MR software (Medis, Leiden, Netherlands) was used to measure PI-ST and LV-WT. The endocardium and epicardium were contoured manually in every LGE-CMR plane. To measure LV-WT accurately, LGE-CMR contours were compared to contours in corresponding Cine-CMR short-axis planes (Figure 1A). Candidate hyperenhanced regions were identified as scar if their mean intensity was >3 standard deviations (SD) above that of remote normal myocardium. Each LGE-CMR short-axis plane was divided into 20 radial sectors. In each sector, 4 radial lines were drawn from epicardium to endocardium and the proportion of each line that intersected scar was calculated.[10] Scar transmurality was defined as the average scar transmurality of all lines per sector (Figure 1B). LV-WT was defined as the average wall thickness of all lines per sector. PI-ST was calculated by the multiplication of scar transmurality and wall thickness. Scar on LGE-CMR was classified by scar transmurality (0%, 1–25%, 26–50%, 51–75%, 76–100%) and intramural scar location (endocardial, transmural, mid wall) (Figure 1C).

Electrophysiological Study

Ventricular programmed-stimulation to induce VT was performed from the right ventricular (RV) apex and outflow tract with up to triple extrastimuli at three basic cycle lengths. If the induced VT sustained without hemodynamic collapse, LV mapping was attempted during VT. Otherwise, substrate mapping was performed during sinus rhythm.

Electroanatomic Maps and Electrogram Characteristics

An EAM system (CARTO, Biosense-Webster, Inc., Diamond Bar, CA) was used to create endocardial maps using a 3.5 mm-tip electrode irrigated ablation catheter (Thermocool, Biosense-Webster, Inc.) during conducted sinus rhythm or ventricular pacing (2 patients). The “Fill Threshold” of the EAM system was set at 15mm. The catheter was inserted into the LV using a trans-septal approach in all patients, followed by heparin administration to maintain an activated clotting time >300 seconds. The LV shell reconstructed from the CMR angiogram was registered to the LV-EAM using landmark registration followed by surface registration. LV apex, mitral, and aortic annulus, or RV septal insertions were selected as landmarks. Additional RV or aortic EAMs were used to minimize rotational error. The accuracy of registration was quantified as the average distance of each EAM point to the closest surface point of the reconstructed LV shell (statistical summation).[22] Bipolar and unipolar EGMs were filtered at 10–400Hz and 1–240Hz, respectively, and voltages were recorded as the difference between the highest and lowest deflections of a stable contact signal. EGM duration and deflection were manually measured from the onset to the end of the EGM deflections at 400mm/s speed. The number of deflections was counted as the summation of both negative and positive deflections in each EGM (Figure 1d).[23] Bipolar EGMs recorded by the distal electrodes of the mapping catheter were categorized by two independent observers as normal, fractionated, isolated potential, and abnormal EGM:[4, 6, 24] 1) normal: sharp biphasic or triphasic spikes with voltage ≥3 mV and duration <70ms, and/or amplitude/duration ratio >0.046, 2) fractionated: voltage ≤0.5mV, duration ≥133ms, and/or amplitude/duration ratio <0.005, 3) isolated potential: a potential separated from the ventricular EGM by an isoelectric segment, and/or a segment with low voltage noise (<0.05 mV) of >20 msec duration at a gain of 40–80 mm/mV, 4) the other EGMs were defined as abnormal EGMs.[24] Discrepancies were resolved by repeat review by a third observer and consensus among all reviewers. To avoid artifact from poor catheter contact, >2 consecutive EGMs with the same morphology were mandated at each accepted EAM point.

Catheter Ablation of Scar-related VT

Ablation targets were determined by pace mapping during sinus rhythm and entrainment mapping during sustained VT. Additional ablations targeted fractionated and isolated potentials, or connected scar to adjacent non-conductive structures (mitral valve annulus). Critical sites of reentrant VT were defined as sites with low voltage and 12/12 ECG morphology match to VT during pacing, or concealed entrainment and post pacing interval minus VT cycle length <30 msec during hemodynamically stable VT. These critical sites were categorized as exit, central pathway, or entrance sites by determination of the ratio of stimulus to QRS time (S-QRS) divided by the VT cycle length (%S-QRS/VT-CL: Exit <30%, Central pathway 30–70%, entrance >70%).[1, 2] Radiofrequency ablations were performed with 40W maximum power for 30–60 seconds at each site. Complete success was defined as non-induciblity of any VT. Partial success was defined as suppression of the clinical VT but induciblity of any other VT. ICD interrogation and reprogramming to original settings was performed immediately after the procedure.

Registration of EAM Points to LGE-CMR Images

LGE-CMR images were retrospectively registered to the endocardial EAM using custom software (Volley, Johns Hopkins University) based on the registration coordinates for EAM merge with the CMR angiogram.[5] Each EAM point was superimposed onto the corresponding region on short-axis LGE-CMR image planes. EGM characteristics corresponding to each image sector on LGE-CMR were recorded as continuous variables.

Statistical Analyses

Continuous variables are expressed as mean ± SD and categorical data as numbers or percentages. Comparisons of continuous variables regarding EGM parameters were made using a nonparametric test based on the distribution of the values. The association of EGM types (normal, abnormal, fractionated and isolated potential) with scar types (Figure 1D) was investigated by the chi-squared test. The association between S-QRS and %S-QRS/VT-CL with scar transmurality was assessed by spearman's correlation test. Multi-level multivariable linear regression models with EGM parameters as dependent variables and an initial full model including LV-WT and PI-ST (as continuous variables), myocardial location (anterior, septal, inferior, lateral), and intramural scar location (endocardial, mid wall, transmural) at each sampled point as independent variables, clustered by patient and adjusting for patient characteristics (age, body mass index (BMI), LV ejection fraction, history of coronary artery bypass and use of antiarrhythmic drugs) were created. The final model for each EGM parameter was selected by backward elimination of the least significant covariates based upon log-likelihood ratio tests of nested models. To obtain estimates of future predictive performance we performed 400 bootstrap repetitions using the Efron-Gong optimism bootstrap, a technique designed to evaluate over-fitting in prediction models. The bootstrap loop included the variable selection methodology entailing a) creation of all possible models using the sampled subset of data and any combination of independent variables, and b) final model selection using the log-likelihood ratio tests of nested models. We also performed leave-one-out cross-validation at the patient level (Supplemental Figure 1). An iteration of leave-one-out cross-validation was used to graphically display the predictive accuracy of non-invasive mapping. Based on measured LV-WT and PI-ST for one patient and the coefficients from the remaining patients, we calculated the predicted bipolar and unipolar voltage, duration, and deflections. The custom software (Volley, Johns Hopkins University)[7] was then used to display each EGM measure on corresponding maps with colors representing the full range of measured data for each EGM parameter. Statistical analyses were performed using STATA (version 12, StataCorp, College Station, Texas) and R statistical software (version 2.15.0, http://www.r-project.org/).

Results

Patients Characteristics

All 23 patients were male and the mean age was 68±8 years. Other baseline characteristics have been summarized in Table 1. Fifteen patients had ICD or biventricular-ICD systems and safely underwent CMR using our protocol.[20] In addition to standard heart failure therapy, antiarrhythmic drugs (amiodarone or sotalol) had been administrated in 18 patients (78.3%). Antiarrhythmic drugs were discontinued ≥3 days prior to VT ablation.

Analyzed sectors on LGE-CMR and EAM Points

A total of 3576 sectors in 189 short-axis LGE-CMR planes of 23 patients' CMR examinations were reviewed. Of these, 2690 sectors (75.2%) were available for quantitative analysis. The remaining sectors (24.8%) were excluded due to MRI susceptibility artifacts in patients with ICD systems. Of 4315 EAM points, 2222 EAM points had to be excluded from the analysis due to the MRI artifacts in corresponding image sectors or evidence of suboptimal catheter contact. Consequently, 2093 EAM points obtained from the LV during sinus rhythm were retrospectively merged with the 2690 analyzable imaging sectors on LGE-CMR. The transmurality and location of scar on all LGE-CMR sectors and those sectors corresponding to sampled points on EAM are summarized in Supplemental Table 1. Compared to the number of sectors with endocardial and transmural scar, mid-wall scar was not frequently observed. Low voltage and dense scar areas defined as <1.5mV and <0.5mV of bipolar voltage covered 29.4% and 6.2% of total LV endocardium on EAM. The LV CMR angiogram shells were successfully merged with the endocardial LV EAM with a mean registration error of 2.8±0.7 mm. Details of electroanatomic mapping and ablation are shown in Supplemental Table 2. Complete success was attained in 10 and partial success in 13 patients. In 2 patients, heart failure exacerbation requiring inpatient diuresis was recognized as a procedural complication.

Comparison of EGM characteristics and Scar Transmurality

The mean bipolar voltage and EGM duration were 3.0±2.3 mV and 96.5±27.0 ms, respectively, in myocardial areas without evidence of scar on LGE-CMR. Bipolar and unipolar EGM voltage measures were inversely associated with endocardial and mid wall scar transmurality ($P<0.0001$ nonparametric test for trend, respectively; Figure 2A, 2B). EGM duration and deflections were positively associated with endocardial and mid wall scar transmurality ($P<0.0001$ nonparametric test for trend, respectively; Figure 2C, 2D). Of all EAM points analyzed, 6.1% had normal EGMs, 29.1% had fractionated EGMs, 3.1% had isolated potentials and 61.7% had abnormal EGMs. There was a positive association between the incidence of fractionated EGM and isolated potentials with endocardial and mid wall scar transmurality ($P<0.0001$ nonparametric test for trend, respectively; Figure 2E). Fractionated EGMs and isolated potentials were more frequently observed in regions with higher scar transmurality.

Comparison of Critical Ablation Sites and Scar Transmurality

A total of 475 radiofrequency applications were delivered. Of all lesions, 7.6%, 21.3%, 27.4%, and 39.1% were delivered to areas with endocardial 1–25%, 26–50%, 51–75%, and 76–100% scar transmurality, respectively (Figure 3A). Additionally, 1.0% and 3.9% were delivered to regions with mid wall scar and no enhancement but adjacent to scar as determined by LGE-CMR. Of 39 reentrant VT critical sites, 17.9%, 20.5% and 61.5% were identified in regions with 26–50% [range: 32–46%], 51–75% [52–74%], and 76–100% [76–100%] scar transmurality, respectively (Figure 3B). The mean scar transmurality in sectors corresponding to VT critical sites was 73±21%. Of all critical sites, 23 sites (59%) were

located within 10 mm of the scar border, and the remaining 41% were in the scar core. Associations were also observed between EGM parameters and EGM types with scar transmurality within critical sites (Figure 3C). S-QRS and %S-QRS/VT-CL were associated with scar transmurality ($P<0.0001$, respectively; Figure 3D). Critical sites with ≥40 msec of S-QRS delay and critical sites with ≥30% of %S-QRS/VT-CL were confined to sectors with >75% scar transmurality.

Predictors of EGM Parameters by Multi-level (Clustered by Patient) Multivariable Linear Regression Analysis

To optimize homogeneity, data from 21 patients with mapping during sinus rhythm was used for multivariable analyses. Using the process of backward elimination, optimal models included myocardial scar location, intramural scar location, LV-WT, and PI-ST for bipolar and unipolar voltage ampltiude; intramural scar location, LV-WT, and PI-ST for deflections; and drug (amiodarone or sotalol), intramural scar location, LV-WT, and PI-ST for electrogram duration. For simplicity, and given the potential confounding effects of age and drug use upon electrogram parameters, we chose to include age, drug, myocardial scar location, intramural scar location, LV-WT, and PI-ST in all models. LV-WT and PI-ST remained independently and significantly associated with each EGM parameter (Table 2). There were also significant associations between myocardial scar location with bipolar and unipolar EGM voltage, intramural scar location with all EGM parameters; and use of antiarrhythmic drugs with EGM duration.

Leave one out cross-validation results have been summarized in Supplemental Figure 1. The top panel of Figure 4 graphically summarizes cross-validation for a single subject. Comparison to the respective invasive EGM parameter maps in the bottom panel of Figure 4 shows excellent qualitative agreement between the predicted and invasive maps. Using 400 bootstrap repetitions with the Efron-Gong optimism bootstrap we obtained median root-mean-squared errors of 1.54 mV (IQR 1.54–1.55 mV), 3.30 mV (IQR 3.26–3.38 mV), 4.17 (IQR 4.05–4.47), and 28.80 msec (IQR 27.83–30.34 msec) for bipolar voltage, unipolar voltage, deflections, and duration respectively. The median overestimation of the model error from the actual error was 0.02 mV (IQR 0.01–0.03 mV), 0.05 mV (IQR 0.02–0.14 mV), 0.13 (IQR 0.00–0.43), and 1.82 msec (IQR 0.85–3.36 msec), respectively.

Discussion

The main findings of this study are that in patients with ischemic cardiomyopathy: (a) after adjusting for patient characteristics, PI-ST and LV-WT are independently associated with local intra-cardiac bipolar and unipolar EGM voltage, duration, and deflections; (b) non-invasive substrate maps can be created using multivariable regression models that summarize the associations between scar on LGE-CMR and EGM parameters on invasive EAM; and (c) critical VT sites are located in areas with >25% scar transmurality and central pathway sites are located in areas with >75% scar transmurality on LGE-CMR.

LV-WT and PI-ST as Independent Predictors of EGM Parameters

Previous reports have described significant associations between PI-ST identified by LGE-CMR,[11–16] pathology[15, 17, 18] or PET-CT[19] and local bipolar and/or unipolar EGM voltage. It is biologically accepted that viable myocardial tissue rather than scar produces the electrical characteristics in each myocardial region. However, previous reports have primarily focused on scar thickness or the ratio of scar to viable tissue rather than LV-WT and PI-ST as independent variables. Our study elucidates the independent significance of LV-WT, PI-ST, and intramural scar location as predictors of EGM signal characteristics and demonstrates that myocardial scar location is a significant determinant of bipolar and

unipolar EGM voltage. Interestingly, EGM duration was significantly associated with antiarrhythmic drug use. This novel finding suggests that EGM duration is affected not only by LV-WT and PI-ST but also by use of medications that contribute to slow myocardial conduction.

Scar Transmurality and EGM Characteristics

Wolf and colleagues demonstrated an association between scar transmurality and bipolar EGM voltage (263 EAM points) in 13 dogs with infarct scar.[17] Our study demonstrates a similar association between scar transmurality and EGM voltage in human myocardium. The positive association between EGM duration and deflections with scar transmurality suggests the existence of slow conduction in regions with higher scar transmurality. Similarly, fractionated EGMs and isolated potentials are positively associated with scar transmurality. Interestingly, the mean bipolar voltage of areas without scar was lower, and EGM duration longer, when compared to results obtained from normal myocardium of patients without structural heart disease (3.0±2.3 mV and 96.5±27.0 msec respectively in our study, versus 6.7±3.4mV and 54±13ms, respectively in patients without structural heart disease). This finding, which is consistent with EAM results from Desjardins et al and Condreanu et al[12, 14] suggests that in patients with ischemic cardiomyopathy even “normal” areas without evidence of scar exhibit alterations in electrophysiological properties.

Scar Transmurality and Critical Sites of Reentrant VT

Previous studies have characterized the EGM characteristics of critical sites necessary for VT initiation and maintenance.[1–4] Our study demonstrates that critical sites are anatomically confined to regions with >25% scar transmurality. Importantly, sites with slow conduction and central pathway VT circuit sites, identified by >40msec of S-QRS[1, 3] and >30% of %S-QRS/VT-CL,[2] localize to regions with >75% scar transmurality. VT circuit exit sites are associated with 25–75% scar transmurality.

Non-Invasive 3D Substrate Maps Based on LGE-CMR

Our study demonstrates that non-invasive LGE-CMR based creation of EGM parameter maps with close approximation of EGM trends in each myocardial region is feasible. Future larger studies with increased EAM point density are necessary to reduce the absolute predictive error. However, some prediction error will always exist, because even with minimal inter-electrode distance, the EGM parameters will vary depending upon the angle and force of catheter-tissue contact. Non-invasive voltage maps have the capacity to mitigate the limited sampling density of endocardial invasive mapping and more closely approximate the underlying substrate. Additionally, non-invasive creation of duration and deflection may provide additional information not currently provided using standard EAM software. Some of this information may also be displayed by scar image integration. Importantly, however, our data shows that not only PI-ST, but also LV-WT (absolute values and not the ratio) predict voltage and other EGM characteristics. In our experience, it is very difficult to accurately display both PI-ST and LV-WT without feature extraction. If the image is transformed to display such information using a color scale, then based upon our data, the transformation process could be used to display more information regarding expected electrogram findings. Incorporation of such data will likely reduce procedural and fluoroscopy time devoted to substrate identification. Importantly, the patients in this study had ischemic cardiomyopathy, severe LV dysfunction, and ICDs prior to ablation procedures; therefore, the data is generalizable to typical patients referred for VT ablation.

Limitations

Our study had a relatively small sample size, which likely led to increased absolute prediction errors, a potential for over-fitting, and an inability to account for multiple subject-level covariates. Antero-apical myocardial regions can exhibit susceptibility artifacts due to field inhomogeneity caused by the ICD in patients with low BMI and/or inferiorly displaced generators.[21] Image artifacts may pose a limitation to use of CMR for ablation guidance in ICD recipients. In this study, 24.8% of the LGE-CMR image sectors were excluded due to ICD susceptibility artifacts. Additionally, 2222 EAM points were excluded from analysis due to registration to an imaging sector with artifact, or evidence of poor catheter contact or stability. These points were excluded based upon a priori set criteria to improve the validity and reproducibility of results. However, their exclusion may have biased the results. Image artifacts were not visualized in sectors included for analysis; however, it is possible that subtle changes in signal intensity exist beyond the visually detectable artifacts and may alter scar border delineation based upon image intensity thresholds. Results may also be limited by a possibility for positional errors when registering EAM points to corresponding sectors on LGE-CMR based on the registration information obtained by the EAM software.[22, 25] The density of EAM sampling was sometimes limited in healthy myocardium. EGM duration and deflection measures depend upon the criteria used for measurement (we employed Tung and colleagues' methodology).[25] Inter-observer reliability analysis was not formally performed. However, disagreements among observers were rare. Finally, EGM parameters on EAM can be affected by the contact or the orientation of the mapping catheter, which may account for some unexplained variance in the models.[26]

Conclusions

LV-WT, PI-ST, and intramural scar location on LGE-CMR of patients with ischemic cardiomyopathy were independently associated with local intra-cardiac bipolar and unipolar EGM voltage, duration and deflections. These associations enable the creation of non-invasive CMR based substrate maps prior to VT ablation. Such maps closely approximate trends in regional measures but not the absolute values of each EGM measure. This novel methodology may improve the safety and efficacy of ablation in patients with ischemic scar-related VT by providing a summary of image details directly useful to the electrophysiologist, reducing procedural time, and mitigating sampling density limitations.

Supplementary Material

Refer to Web version on PubMed Central for supplementary material.

Acknowledgments

Funding Sources: Dr. Sasaki is funded by the Francis Chiaramonte MD Private Foundation. Dr. Nazarian is supported by Grant K23HL089333 and Dr. Halperin by Grant R01-HL094610 from the National Institutes of Health.

References

1. Stevenson WG, Khan H, Sager P, Saxon LA, Middlekauff HR, Natterson PD, Wiener I. Identification of reentry circuit sites during catheter mapping and radiofrequency ablation of ventricular tachycardia late after myocardial infarction. Circulation. 1993; 88:1647–1670. [PubMed: 8403311]
2. Hsia HH, Lin D, Sauer WH, Callans DJ, Marchlinski FE. Anatomic characterization of endocardial substrate for hemodynamically stable reentrant ventricular tachycardia: Identification of endocardial conducting channels. Heart Rhythm. 2006; 3:503–512. [PubMed: 16648052]

3. Stevenson WG, Sager PT, Natterson PD, Saxon LA, Middlekauff HR, Wiener I. Relation of pace mapping qrs configuration and conduction delay to ventricular tachycardia reentry circuits in human infarct scars. J Am Coll Cardiol. 1995; 26:481–488. [PubMed: 7608454]
4. Bogun F, Good E, Reich S, Elmouchi D, Igic P, Lemola K, Tschopp D, Jongnarangsin K, Oral H, Chugh A, Pelosi F, Morady F. Isolated potentials during sinus rhythm and pace-mapping within scars as guides for ablation of post-infarction ventricular tachycardia. J Am Coll Cardiol. 2006; 47:2013–2019. [PubMed: 16697318]
5. Estner HL, Zviman MM, Herzka D, Miller F, Castro V, Nazarian S, Ashikaga H, Dori Y, Berger RD, Calkins H, Lardo AC, Halperin HR. The critical isthmus sites of ischemic ventricular tachycardia are in zones of tissue heterogeneity, visualized by magnetic resonance imaging. Heart Rhythm. 2011; 8:1942–1949. [PubMed: 21798226]
6. Marchlinski FE, Callans DJ, Gottlieb CD, Zado E. Linear ablation lesions for control of unmappable ventricular tachycardia in patients with ischemic and nonischemic cardiomyopathy. Circulation. 2000; 101:1288–1296. [PubMed: 10725289]
7. Kim RJ, Fieno DS, Parrish TB, Harris K, Chen EL, Simonetti O, Bundy J, Finn JP, Klocke FJ, Judd RM. Relationship of mri delayed contrast enhancement to irreversible injury, infarct age, and contractile function. Circulation. 1999; 100:1992–2002. [PubMed: 10556226]
8. Setser RM, Bexell DG, O'Donnell TP, Stillman AE, Lieber ML, Schoenhagen P, White RD. Quantitative assessment of myocardial scar in delayed enhancement magnetic resonance imaging. J Magn Reson Imaging. 2003; 18:434–441. [PubMed: 14508780]
9. Roes SD, Borleffs CJ, van der Geest RJ, Westenberg JJ, Marsan NA, Kaandorp TA, Reiber JH, Zeppenfeld K, Lamb HJ, de Roos A, Schalij MJ, Bax JJ. Infarct tissue heterogeneity assessed with contrast-enhanced mri predicts spontaneous ventricular arrhythmia in patients with ischemic cardiomyopathy and implantable cardioverter-defibrillator. Circ Cardiovasc Imaging. 2009; 2:183–190. [PubMed: 19808591]
10. Nazarian S, Bluemke DA, Lardo AC, Zviman MM, Watkins SP, Dickfeld TL, Meininger GR, Roguin A, Calkins H, Tomaselli GF, Weiss RG, Berger RD, Lima JA, Halperin HR. Magnetic resonance assessment of the substrate for inducible ventricular tachycardia in nonischemic cardiomyopathy. Circulation. 2005; 112:2821–2825. [PubMed: 16267255]
11. Perin EC, Silva GV, Sarmento-Leite R, Sousa AL, Howell M, Muthupillai R, Lambert B, Vaughn WK, Flamm SD. Assessing myocardial viability and infarct transmurality with left ventricular electromechanical mapping in patients with stable coronary artery disease: Validation by delayed-enhancement magnetic resonance imaging. Circulation. 2002; 106:957–961. [PubMed: 12186800]
12. Codreanu A, Odille F, Aliot E, Marie PY, Magnin-Poull I, Andronache M, Mandry D, Djaballah W, Regent D, Felblinger J, de Chillou C. Electroanatomic characterization of post-infarct scars comparison with 3-dimensional myocardial scar reconstruction based on magnetic resonance imaging. J Am Coll Cardiol. 2008; 52:839–842. [PubMed: 18755347]
13. Wijnmaalen AP, van der Geest RJ, van Huls van Taxis CF, Siebelink HM, Kroft LJ, Bax JJ, Reiber JH, Schalij MJ, Zeppenfeld K. Head-to-head comparison of contrast-enhanced magnetic resonance imaging and electroanatomical voltage mapping to assess post-infarct scar characteristics in patients with ventricular tachycardias: Real-time image integration and reversed registration. Eur Heart J. 2011; 32:104–114. [PubMed: 20864488]
14. Desjardins B, Crawford T, Good E, Oral H, Chugh A, Pelosi F, Morady F, Bogun F. Infarct architecture and characteristics on delayed enhanced magnetic resonance imaging and electroanatomic mapping in patients with postinfarction ventricular arrhythmia. Heart Rhythm. 2009; 6:644–651. [PubMed: 19389653]
15. Psaltis PJ, Carbone A, Leong DP, Lau DH, Nelson AJ, Kuchel T, Jantzen T, Manavis J, Williams K, Sanders P, Gronthos S, Zannettino AC, Worthley SG. Assessment of myocardial fibrosis by endoventricular electromechanical mapping in experimental nonischemic cardiomyopathy. Int J Cardiovasc Imaging. 2011; 27:25–37. [PubMed: 20585861]
16. Dickfeld T, Tian J, Ahmad G, Jimenez A, Turgeman A, Kuk R, Peters M, Saliaris A, Saba M, Shorofsky S, Jeudy J. Mri-guided ventricular tachycardia ablation: Integration of late gadolinium-enhanced 3d scar in patients with implantable cardioverter-defibrillators. Circ Arrhythm Electrophysiol. 2011; 4:172–184. [PubMed: 21270103]

17. Wolf T, Gepstein L, Dror U, Hayam G, Shofti R, Zaretzky A, Uretzky G, Oron U, Ben-Haim SA. Detailed endocardial mapping accurately predicts the transmural extent of myocardial infarction. J Am Coll Cardiol. 2001; 37:1590–1597. [PubMed: 11345370]

18. Reddy VY, Wrobleski D, Houghtaling C, Josephson ME, Ruskin JN. Combined epicardial and endocardial electroanatomic mapping in a porcine model of healed myocardial infarction. Circulation. 2003; 107:3236–3242. [PubMed: 12796129]

19. Dickfeld T, Lei P, Dilsizian V, Jeudy J, Dong J, Voudouris A, Peters R, Saba M, Shekhar R, Shorofsky S. Integration of three-dimensional scar maps for ventricular tachycardia ablation with positron emission tomography-computed tomography. JACC Cardiovasc Imaging. 2008; 1:73–82. [PubMed: 19356409]

20. Nazarian S, Hansford R, Roguin A, Goldsher D, Zviman MM, Lardo AC, Caffo BS, Frick KD, Kraut MA, Kamel IR, Calkins H, Berger RD, Bluemke DA, Halperin HR. A prospective evaluation of a protocol for magnetic resonance imaging of patients with implanted cardiac devices. Ann Intern Med. 2011; 155:415–424. [PubMed: 21969340]

21. Sasaki T, Hansford R, Zviman MM, Kolandaivelu A, Bluemke DA, Berger RD, Calkins H, Halperin HR, Nazarian S. Quantitative assessment of artifacts on cardiac magnetic resonance imaging of patients with pacemakers and implantable cardioverter-defibrillators. Circ Cardiovasc Imaging. 2011; 4:662–670. [PubMed: 21946701]

22. Bertaglia E, Brandolino G, Zoppo F, Zerbo F, Pascotto P. Integration of three-dimensional left atrial magnetic resonance images into a real-time electroanatomic mapping system: Validation of a registration method. Pacing Clin Electrophysiol. 2008; 31:273–282. [PubMed: 18307621]

23. Tung R, Josephson ME, Reddy V, Reynolds MR. Influence of clinical and procedural predictors on ventricular tachycardia ablation outcomes: An analysis from the substrate mapping and ablation in sinus rhythm to halt ventricular tachycardia trial (smash-vt). J Cardiovasc Electrophysiol. 2010; 21:799–803. [PubMed: 20132389]

24. Josephson, ME. Clinical cardiac electrophysiology: Techniques and interpretations. Philadelphia: Lippincott Williams & Wilkins; 2002.

25. Tung R, Nakahara S, Ramirez R, Lai C, Fishbein MC, Shivkumar K. Distinguishing epicardial fat from scar: Analysis of electrograms using high-density electroanatomic mapping in a novel porcine infarct model. Heart Rhythm. 2010; 7:389–395. [PubMed: 20185114]

26. Otomo K, Uno K, Fujiwara H, Isobe M, Iesaka Y. Local unipolar and bipolar electrogram criteria for evaluating the transmurality of atrial ablation lesions at different catheter orientations relative to the endocardial surface. Heart Rhythm. 2010; 7:1291–1300. [PubMed: 20541040]

Radiofrequency catheter ablation is a useful to reduce episodes of sustained monomorphic ventricular tachycardia (VT) in patients with implantable defibrillators and prior myocardial infarction. Hemodynamically instability often limits mapping during VT and identification of potential reentry circuit substrate by mapping during sinus or paced rhythm is often used to guide ablation in these patients. We sought to quantify the association of reentry circuit sites with magnetic resonance myocardial image characteristics to gain insights regarding the anatomy of tissues and critical sites that support post-infarct VT. In a series of 23 patients, we found that critical VT sites were associated with >25% scar transmurality and central VT circuit sites were associated with >75% scar transmurality. Additionally, left ventricular wall thickness, post-infarct scar thickness, and intramural scar location were associated with local intra-cardiac electrogram amplitudes, duration and deflections. These findings demonstrate the feasibility of creating non-invasive image based maps prior to the procedure, which can potentially be used to guide VT substrate ablation.

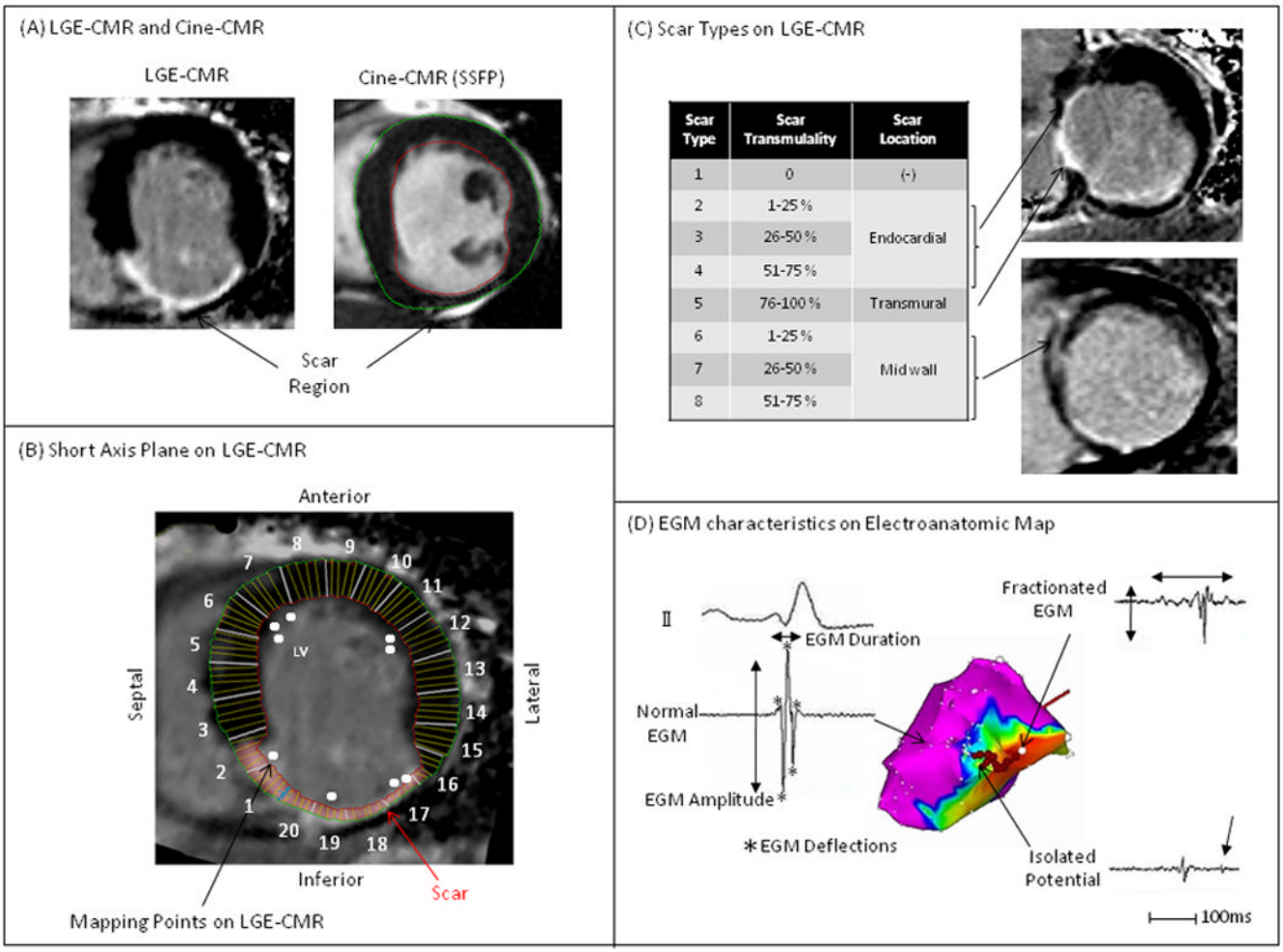

Figure 1.

(A) Scar was identified by LGE-CMR. PI-ST and LV-WT were determined by both LGE-CMR and Cine-CMR. (B) Mapping points on EAM were registered to the corresponding region on short-axis planes of LGE-CMR. (C) Scar on LGE-CMR was divided into 8 types by scar transmurality (PI-ST/LV-WT = 0–25, 26–50, 51–75, or 76–100%) and intramural scar location (normal, endocardial, mid wall, transmural). (D) EGM characteristics on EAM were defined as EGM parameters (bipolar and unipolar EGM voltages, duration, deflections) and EGM types (normal, fractionated EGM, isolated potential, abnormal EGM).

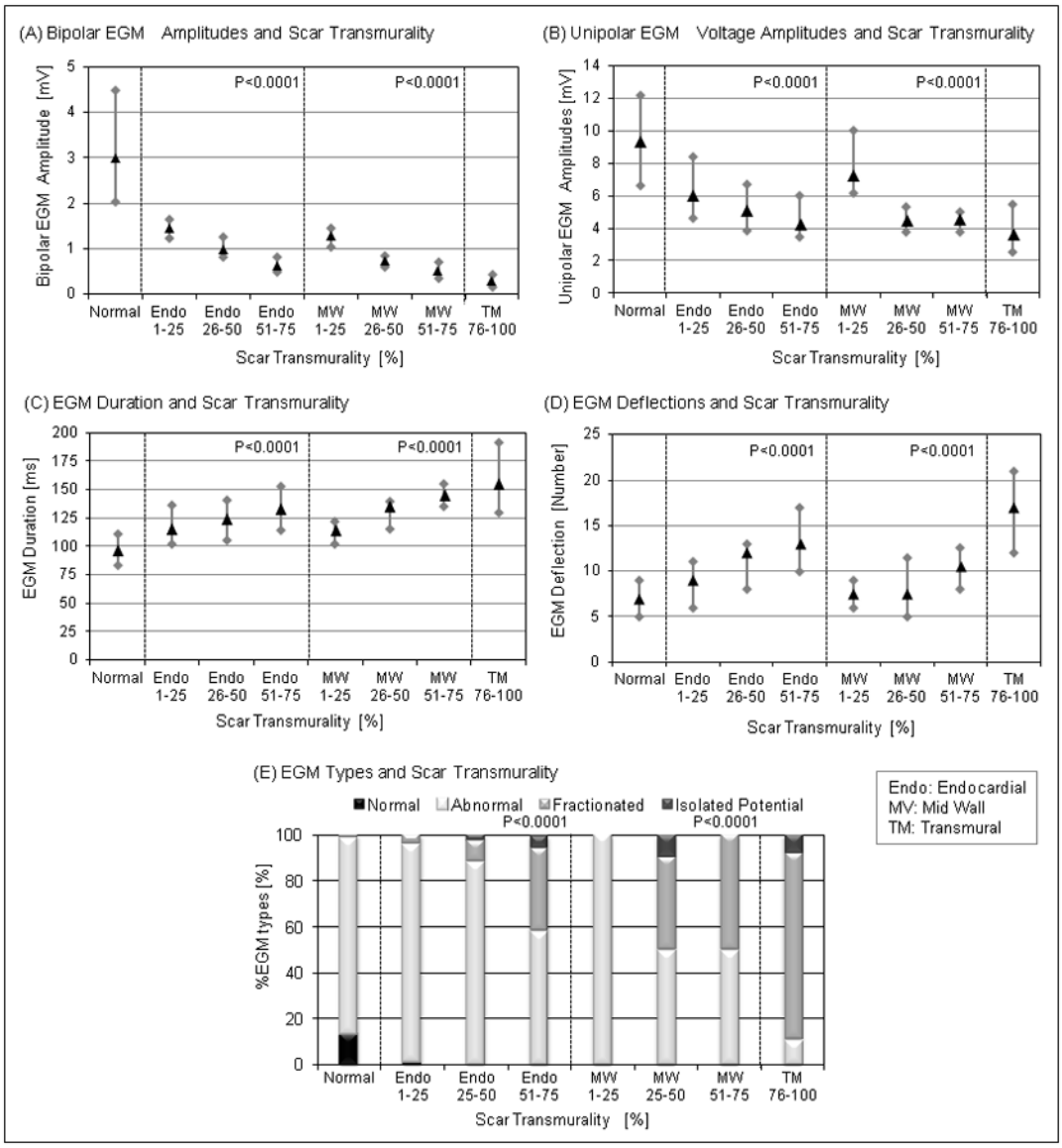

Figure 2.

The association of EGM parameters or EGM types with scar transmurality. (A) Bipolar and unipolar EGM voltage amplitudes were negatively associated with endocardial (P<0.0001) and mid wall scar transmurality (P<0.0001). (B) EGM duration and deflections were positively associated with endocardial (P<0.0001) and mid wall scar transmurality (P<0.0001). The Box plots show the interquartile range (grey bar) and the median (black triangle). (C) Fractionated and isolated potential were more frequently observed in scar regions with greater scar transmurality (P<0.0001).

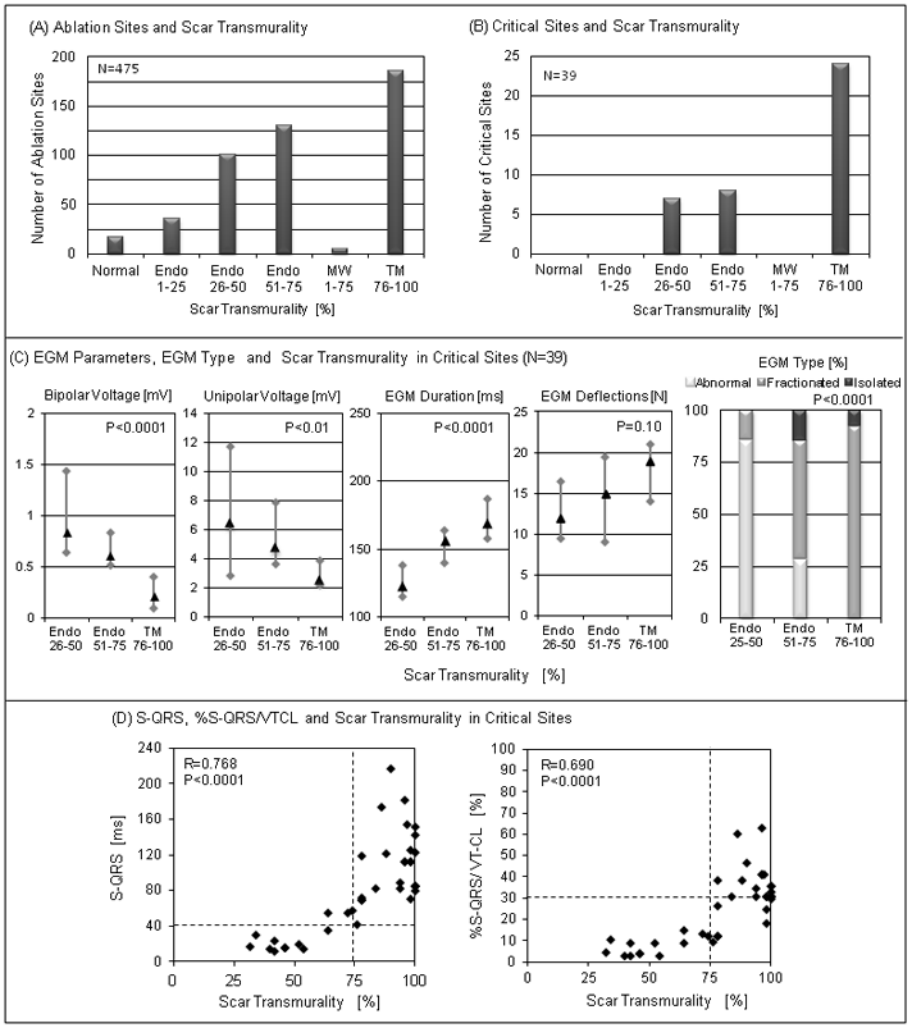

Figure 3.

The association of ablation sites and critical VT sites with scar transmurality. (A) Ablation sites were observed in regions with scar and normal myocardium adjacent to the scar. (B) Critical sites were identified only in scar region with >25% scar transmurality. (C) Significant associations among EGM parameters and EGM types with scar transmurality were observed (except EGM deflections) within critical sites. (D) S-QRS (R=0.768, P<0.0001) and %S-QRS/VT-CL (R=0.690, P<0.0001) were significantly associated with scar transmurality. Critical sites with ≥40 msec of S-QRS and ≥30% of %S-QRS/VT-CL were identified by >75% scar transmurality.

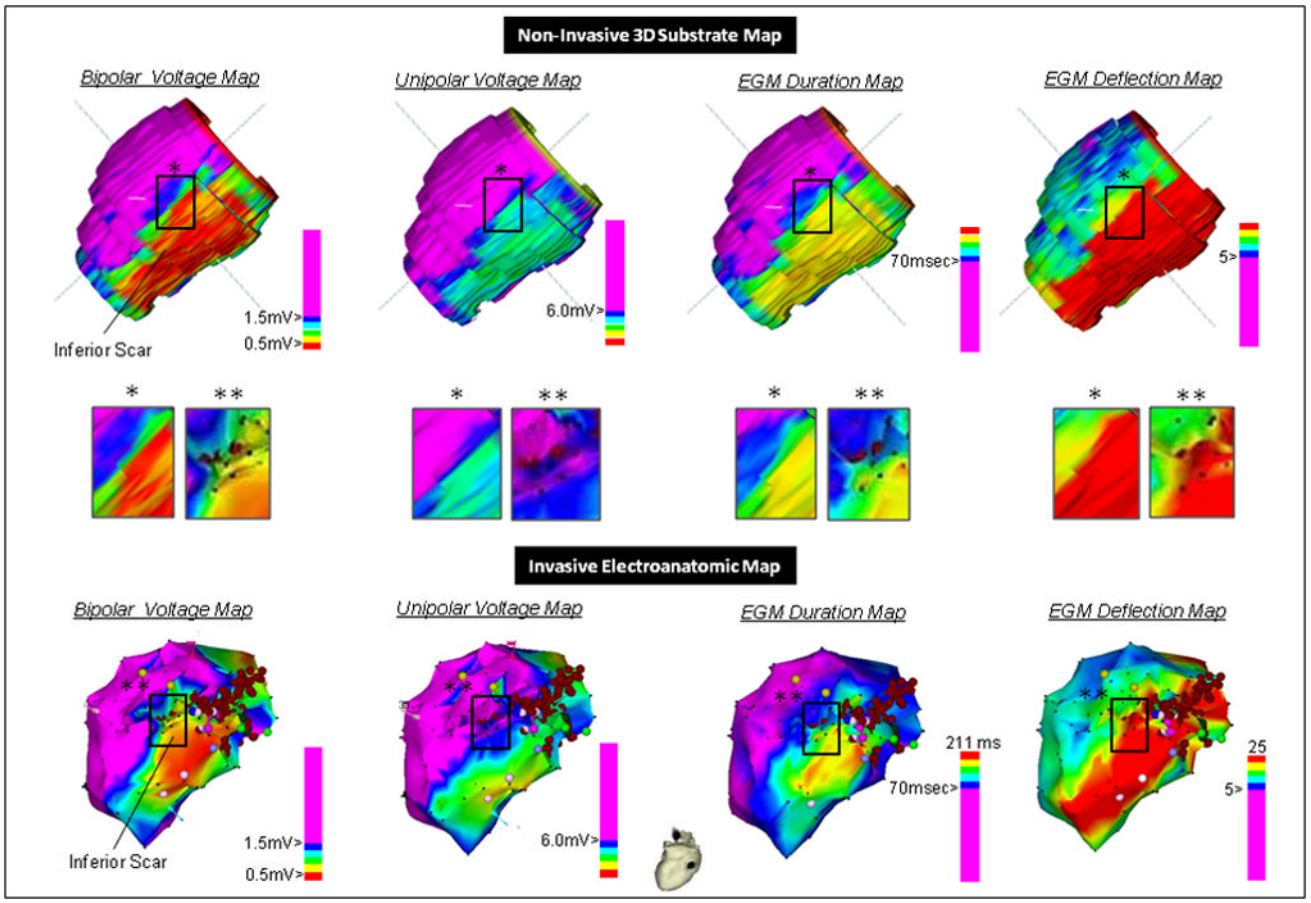

Figure 4.

Qualitative comparison of the invasive versus non-invasive substrate map created using LV-WT and post-infarct scar thickness (PI-ST) on LGE-CMR, and a single iteration of the leave one cross-validation methodology. Upper panel: Leave one out cross-validation substrate map results for bipolar and unipolar EGM voltage, duration and deflections. Middle panel: Higher resolution qualitative comparison of the non-invasive map with invasive maps in image subsets. The resolution of the non-invasive maps (1.5×1.2×8 mm) was higher than that of invasive maps obtained by point-by-point mapping; therefore, minute differences in image characteristics of the predicted map versus the invasive map may be due to extrapolation of each “real” electrogram to nearby areas on the invasive map. Lower panel: Invasive EAMs of bipolar and unipolar voltage, duration and deflection and ablation points (red points). The EAM system does not provide duration and deflection maps routinely, the invasive duration and deflection measures were manually entered for each 3-dimensional location for color display and comparison to the predicted maps.

Table 1

Patient Characteristics

	N=23
Age [years]	69 [59–72]
Gender Male/Female	23/0
BMI [kg/m2]	26.4 [24.0–29.6]
HBP/DLP/DM/smoking	17/12/4/10
History of CABG	10
Myocardial Infarction	
Anteroseptal/Inferior/lateral/Broad	7/12/2/2
Ventricular Tachycardia (VT)	
Stable/Unstable	9/14
Monomorphic/Pleomorphic	9/14
Use of Antiarrhythmic Drug	
None/Amiodarone/Sotalol	5/15/3
MRI with In-situ ICD	15
ICD/BiV-ICD	12/3
Echocardiography	
Ejection Fraction [%]	33 [25–43]
Left Ventricular Diastolic Diameter [mm]	56 [51–60]
MRI	
LV End-diastolic volume [ml]	247 [205–324]
LV End-systolic volume [ml]	171 [123–240]
LV Stroke Volume [ml/beat]	85 [77–90]
LV Cardiac Output [ml/minute]	4.9 [4.4–6.1]
LV Ejection Fraction [%]	30 [26–40]

Categorical values are represented as numbers and continuous variables as median [interquartile range].

BMI=body mass index; HBP=high blood pressure; DLP=dyslipidemia; DM=diabetes mellitus; CABG=coronary artery bypass grafting; ICD=implantable cardioverter defibrillator; LV=left ventricle.

Table 2

Multivariable Multi-Level Linear Regression Analysis (clustered by patient) for 21 Patients with Mapping During Sinus Rhythm

Independent Variables		Electrogram Parameters							
		Bipolar Voltage (mV)		Unipolar Voltage (mV)		Duration (msec)		Deflections (number)	
		B	P	B	P	B	P	B	P
LV Wall Thickness (mm)		**0.419**	**<0.001**	**0.685**	**<0.001**	**−3.132**	**<0.001**	**−0.713**	**<0.001**
Post-infarct Scar Thickness (mm)		**−0.265**	**<0.001**	**−0.192**	**0.016**	**1.724**	**0.026**	**0.622**	**<0.001**
Myocardial Scar Location (Septum as Reference)	Anterior	0.178	0.124	**1.222**	**<0.001**	−0.323	0.888	0.009	0.978
	Lateral	**0.813**	**<0.001**	**0.744**	**<0.001**	−1.581	0.391	−0.031	0.903
	Inferior	**0.822**	**<0.001**	0.225	0.297	2.741	0.192	0.171	0.557
Intramural Scar Location (No Scar as Reference)	Endocardial	**−0.568**	**<0.001**	**−1.970**	**<0.001**	**18.176**	**<0.001**	0.723	0.129
	Mid-Wall	**−1.441**	**<0.001**	**−3.488**	**<0.001**	**19.874**	**<0.001**	−0.969	0.203
	Transmural	−0.135	0.592	**−1.831**	**<0.001**	**39.335**	**<0.001**	**2.179**	**0.002**
Anti-arrhythmic Drug Use (No drug as Reference)	Amiodarone	−0.152	0.240	−0.872	0.238	**15.486**	**0.019**	1.711	0.133
	Sotalol	0.375	0.123	−1.049	0.412	**33.835**	**0.003**	3.750	0.055
Age		0.004	0.553	0.037	0.397	−0.015	0.970	0.063	0.337

Significant regression coefficients and P-values defined as P<0.05 are highlighted in bold font.

B=regression coefficients; P=P-value. Abbreviations listed with Table 1.